

# Fluid Vesicles with Viscous Membranes in Shear Flow

Hiroshi Noguchi and Gerhard Gompper

*Institut für Festkörperforschung, Forschungszentrum Jülich, 52425 Jülich, Germany*

The effect of membrane viscosity on the dynamics of vesicles in shear flow is studied. We present a new simulation technique, which combines three-dimensional multi-particle collision dynamics for the solvent with a dynamically-triangulated membrane model. Vesicles are found to transit from steady tank-treading to unsteady tumbling motion with increasing membrane viscosity. Depending on the reduced volume and membrane viscosity, shear can induce both discocyte-to-prolate and prolate-to-discocyte transformations. This dynamical behavior can be understood from a simplified model.

PACS numbers: 87.16.Dg, 47.55.-t, 87.17.Aa

The dynamical behavior of vesicles — closed lipid membranes in aqueous solution — under shear flow is an important subject not only of fundamental research but also in medical applications. For example, in microcirculation, the deformation of red blood cells reduces the flow resistance of microvessels. In diseases such as diabetes mellitus and sickle cell anemia, red blood cells have reduced deformability and often block microvascular flow. Although red blood cells do not have a nucleus and other intracellular organelles, they are of more complex than simple lipid vesicles, since their plasma membrane has an attached spectrin network, which modifies its elastic and rheological properties. The deformability of cells and vesicles is determined by their shape, the viscosity of the internal fluid, and the viscoelasticity of the membrane [1].

The dynamical behavior of vesicles in shear flow has been studied experimentally [1, 2], theoretically [3, 4], and numerically [5, 6, 7]. The vesicle shape is determined by the competition of the curvature elasticity of the membrane, the constraints of constant volume  $V$  and constant surface area  $S$ , and the external hydrodynamic forces. One of the difficulties in theoretical studies of the hydrodynamic effects on the vesicle dynamics is the boundary condition for the embedding fluid on the vesicle surface, which changes its shape dynamically. In some previous studies, a fluid vesicle was therefore modeled as an ellipsoid with fixed shape [3]. More recently, the time-evolution of the shape was studied numerically using a boundary integral method in three spatial dimensions [5] or an advected-field method in two spatial dimensions [6]. The red blood cell membrane has also been modeled as an elastic capsule of discocyte shape [7].

Two types of dynamics have been found in these studies, a steady state with a tank-treading motion of the membrane and a finite inclination angle with the flow direction, and an unsteady state with a tumbling (flipping) motion. A transition from tank-treading to tumbling motion with an increasing viscosity of the internal fluid has been predicted for fluid vesicles with fixed ellipsoidal shape in three dimensions [3], and with the advected-field method in two dimensions [6]. When the

shape is relaxed dynamically in three dimensions, all discocyte vesicles were surprisingly found to transform into prolates in shear flow, even for the smallest shear rates studied [5].

In this letter, we focus on the effect of the membrane viscosity on the dynamics of vesicles in shear flow. This is an important question, because the membrane of red blood cells, for example, becomes more viscous on aging [4, 8] or in diabetes mellitus [9]. Experiments indicate that the energy dissipation in the membrane is larger than that inside a red blood cell [4]. Furthermore, it has been shown recently that vesicles can not only be made from lipid bilayers, but also from bilayers of block copolymers [10]. These “polymersomes” have been shown to have a membrane viscosity which is several orders of magnitude larger than for liposomes [11].

Several mesoscopic simulation techniques for fluid flow have been developed in recent years. We present here the first simulation studies for a combination of mesoscopic model for the solvent and a coarse-grained, dynamically-triangulated surface model for the membrane. This approach has four main advantages: (i) The membrane is described explicitly, so that their properties like the viscosity can be varied easily; (ii) thermal fluctuation of both the solvent and the membrane are fully and consistently taken into account; (iii) the method can easily be generalized to more complex flow geometries; and (iv) no numerical instabilities can occur.

We employ a particle-based hydrodynamics method [12, 13, 14, 15, 16, 17, 18] to simulate the solvent, which is called multi-particle collision dynamics (MPCD) [17, 18] or stochastic rotation dynamics [14, 15]. This method was applied, for example, to flow around a solid object [17] and to polymer dynamics [13, 18]. The fluids in the interior and exterior of the vesicle are taken to be the same, in particular to have the same viscosity  $\eta_0$ .

As the MPCD model is described in detail in Refs. [12, 13, 14, 15], we can be very brief in explaining the mesoscopic simulation technique. The solvent is described by  $N_s$  point-like particles of mass  $m_s$  moving in a rectangular box of size  $L_x \times L_y \times L_z$ . The algorithm consists of alternating streaming and collision steps. In the stream-

ing step, the particles move ballistically and the position of each particle  $\mathbf{r}_i$  is updated according to

$$\mathbf{r}_i(t+h) = \mathbf{r}_i(t) + \mathbf{v}_i(t)h, \quad (1)$$

where  $\mathbf{v}_i$  is the velocity of particle  $i$  and  $h$  is the time interval between collisions. In the collision step, the particles are sorted into cubic cells of lattice constant  $a$ . The collision step consists of a stochastic rotation of the relative velocities of each particle in a cell,

$$\mathbf{v}_i(t) = \mathbf{v}_{\text{cm}}(t) + \mathbf{\Omega}(\varphi)(\mathbf{v}_i(t) - \mathbf{v}_{\text{cm}}(t)), \quad (2)$$

where  $\mathbf{v}_{\text{cm}}$  is the velocity of the center of mass of all particles in the cell. The matrix  $\mathbf{\Omega}(\varphi)$  rotates velocities by a fixed angle  $\varphi$  around an axis, which is chosen randomly for each cell. In our simulation, the angle  $\varphi = \pi/2$  is employed. We apply a random-shift procedure [14] before each collision step to ensure Galilean invariance.

For the membrane, we employ a dynamically-triangulated surface model [19], in which the membrane is described by  $N_{\text{mb}}$  vertices which are connected by tethers to form a triangular network. The vertices have excluded volume and mass  $m_{\text{mb}}$ . The shapes and fluctuations of the membrane are controlled by curvature elasticity with the energy [20],

$$H_{\text{cv}} = \frac{\kappa}{2} \int (C_1 + C_2)^2 dS, \quad (3)$$

where  $\kappa$  is the bending modulus, and  $C_1$  and  $C_2$  are the principal curvatures at each point of the membrane. The curvature energy is discretized as described in Ref. [21]. To model the fluidity of the membrane, tethers can be flipped between the two possible diagonals of two adjacent triangles. These bond flips provide also a convenient way to vary the membrane viscosity  $\eta_{\text{mb}}$ , because it increases with decreasing bond-flip rate. In contrast to previous studies of dynamically triangulated surfaces, which were all done by Monte Carlo simulations, we introduce a smooth bond-interaction potential, which makes the model amenable for molecular dynamics simulations.

The solvent particles interact with the membrane in two ways. First, the membrane vertices are included in the MPCD collision procedure [13]. Second, the solvent particles are scattered elastically or via bounce-back from membrane triangles. We use here the procedure suggested in Ref. [16] for a spherical particle.

To induce a shear flow, we employed Lee-Edwards boundary condition [15, 22], which gives a linear flow profile  $(v_x, v_y, v_z) = (\dot{\gamma}z, 0, 0)$  in the MPCD fluid. The particle density was set to  $\rho = 10m_s/a^3$  ( $N_s = 450000$ ,  $L_x = 50a$ ,  $L_y = L_z = 30a$ ). In experimental conditions of red blood cells and liposomes, the Reynolds number  $\text{Re} = \dot{\gamma}\rho R_0^2/\eta_0$  is very small ( $\text{Re} \sim 10^{-3}$ ), where  $R_0 = \sqrt{S/4\pi}$  is the effective vesicle radius. Therefore, we chose a short mean free path  $h\sqrt{k_B T/m_s} = 0.025a$ ,

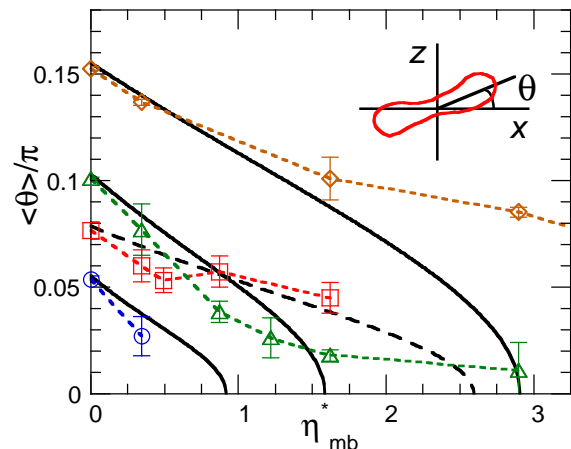


FIG. 1: (Color online) Dependence of the average inclination angle  $\langle \theta \rangle$  ( $-\pi/2 \leq \theta < \pi/2$ ) on the membrane viscosity  $\eta_{\text{mb}}^*$  for reduced shear rate  $\dot{\gamma}^* = 0.92$  and various reduced volumes  $V^*$ . The error bars are estimated from three independent runs. Squares and circles represent discocyte and prolate vesicles at  $V^* = 0.59$ , respectively. Triangles and diamonds represent prolate vesicles at  $V^* = 0.78$  and  $V^* = 0.91$ , where the prolate is the only stable shape. The solid lines and broken line are calculated by K-S theory with prolate ( $V^* = 0.59, 0.78$ , and  $0.91$ ) and oblate ellipsoids ( $V^* = 0.59$ ), respectively.

where  $k_B$  is the Boltzmann constant and  $T$  is the temperature [18]. Then the viscosity of solvent fluid is  $\eta_0 = 20.1\sqrt{m_s k_B T}/a^2$  [15]. We used  $\kappa = 20k_B T$ ,  $N_{\text{mb}} = 500$ , and  $m_{\text{mb}} = 10m_s$ . The volume  $V$  and surface area  $S = 405a^2$  of a vesicle are kept constant to about 1% accuracy. With these parameters, we obtain a Reynolds number  $\text{Re} \simeq 0.1$ . The results are conveniently expressed in terms of dimensionless variables: the reduced volume  $V^* = V/(4\pi R_0^3/3)$ , the intrinsic time scale  $\tau = \eta_0 R_0^3/\kappa$ , the reduced shear rate  $\dot{\gamma}^* = \dot{\gamma}\tau$ , and the relative membrane viscosity  $\eta_{\text{mb}}^* = \eta_{\text{mb}}/\eta_0 R_0$ . Details of the numerical scheme will be published elsewhere [23].

At  $\eta_{\text{mb}}^* = 0$ , a vesicle exhibits tank-treading motion for all simulated reduced volumes in the range  $0.59 \leq V^* \leq 0.97$ . We calculated the average inclination angles  $\langle \theta \rangle$ , and found them to agree very well with those obtained by the boundary integral method [5].

With increasing membrane viscosity  $\eta_{\text{mb}}^*$ , the inclination angle  $\theta$  decreases, as shown in Fig. 1. The qualitative features of the simulation data are reproduced very well by the theory of Keller and Skalak (K-S) [3, 4]. Note that there are no adjustable parameters. Due to the approximations in the K-S theory, an agreement on a quantitative level cannot be expected: (i) an ellipsoidal shape is assumed, which is only mimics the real shapes of vesicles, (ii) the flow on the surface of the droplet is not locally area conserving, as it must be for an incompressible membrane, and (iii) thermal fluctuations are ignored in the theory, but are present in the simulations. In the K-S

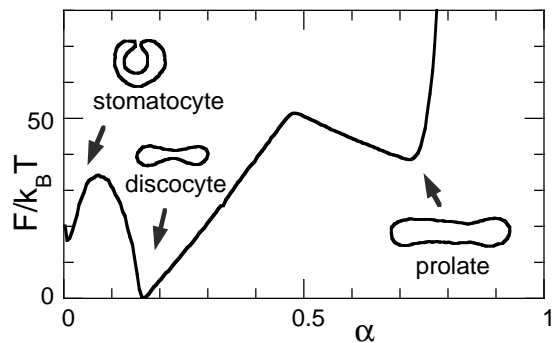


FIG. 2: Free-energy profile  $F(\alpha)$  of the asphericity  $\alpha$  for  $V^* = 0.59$  in the absence of shear flow. The sliced snapshots of stable (discocyte) and metastable (prolate and stomatocyte) shapes are also shown.

theory, the vesicle transits from tank-treading to tumbling motion when the angle  $\theta$  reaches 0. In contrast, we observe tumbling intermittently to occur already for nonzero  $\langle\theta\rangle$ , since our simulation includes thermal fluctuation. For example, the vesicle with  $V^* = 0.78$  starts tumbling at  $\eta_{\text{mb}}^* = 1.22$ . This intermittent tumbling smoothes out the decrease in  $\langle\theta\rangle$  around the transition point, compare Fig. 1.

We now focus on the case  $V^* = 0.59$ . At this reduced volume, the oblate discocyte shape is stable and the prolate and stomatocyte shapes are metastable in the absence of shear flow. Fig. 2 shows the free energy  $F$  as a function of the asphericity  $\alpha$ , calculated with a version of the generalized-ensemble Monte Carlo method [24]. The asphericity  $\alpha = [(\lambda_1 - \lambda_2)^2 + (\lambda_2 - \lambda_3)^2 + (\lambda_3 - \lambda_1)^2] / [2R_{\text{g}}^4]$ , with the eigenvalues  $\lambda_1 \leq \lambda_2 \leq \lambda_3$  of the moment-of-inertia tensor and the squared radius of gyration  $R_{\text{g}}^2 = \lambda_1 + \lambda_2 + \lambda_3$ , is a convenient measure to distinguish oblate and prolate shapes, where  $\alpha = 0$  for spheres,  $\alpha = 1$  for thin rods, and  $\alpha = 0.25$  for thin discs [25]. The shear flow changes this stability. For membrane viscosity  $\eta_{\text{mb}}^* = 0$  and shear rates  $\dot{\gamma}^* \geq 1.66$ , the discocyte state is found to be destabilized and to transform into a prolate, in agreement with the results of Ref. [5]. However, for a smaller shear rate of  $\dot{\gamma}^* = 0.92$ , the discocyte vesicle retains its shape. Speculations about shear to be a singular perturbation [5] can therefore be ruled out.

The inclination angle  $\theta$  of prolates decreases faster than that of discocytes with increasing  $\eta_{\text{mb}}^*$ , see Fig. 1. At a large membrane viscosity of  $\eta_{\text{mb}}^* = 1.62$ , the prolate enters the tumbling phase, while the discocyte remains in the tank-treading phase. The reason is that the discocyte has a flat dimple region and is less affected by the membrane viscosity than the prolate. Remarkably, for small shear rates  $\dot{\gamma}^* \leq 1.84$ , the (metastable) prolate starts tumbling, but after a  $\pi$  or  $2\pi$  rotation, transforms into a tank-treading discocyte, see Fig. 3. Only for larger shear rates of  $\dot{\gamma}^* \geq 2.76$ , the tumbling continues — ac-

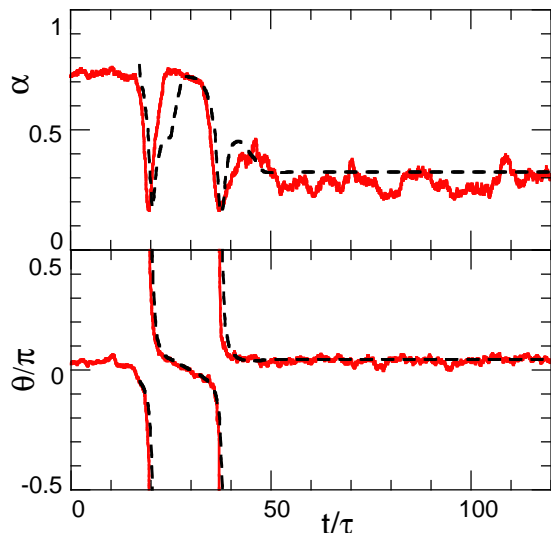


FIG. 3: (Color online) Time development of (a) asphericity  $\alpha$  and (b) inclination angle  $\theta$ , for  $V^* = 0.59$ ,  $\eta_{\text{mb}}^* = 1.62$  and  $\dot{\gamma}^* = 1.84$ . The broken lines are obtained from Eqs. (4) and (5) with  $\zeta_\alpha = 100$ ,  $A = 15$ , and  $B(\alpha) = 1.1 - 0.18\alpha$ .

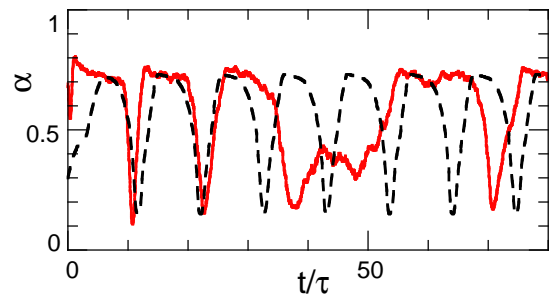


FIG. 4: (Color online) Time development of (a) asphericity  $\alpha$  and (b) inclination angle  $\theta$  at  $\dot{\gamma}^* = 2.76$ . The other parameters are set to same values in Fig. 3.

companied by shape oscillations between prolate and discocyte (Fig. 4). At intermediate membranes viscosities,  $\eta_{\text{mb}}^* = 0.49$  and  $\eta_{\text{mb}}^* = 0.87$ , and shear rate  $\dot{\gamma}^* = 0.92$ , the prolate transforms into a discocyte after tank-treading motion for a time of  $(70 \pm 40)\tau$  or  $(40 \pm 20)\tau$  by thermal fluctuation, respectively. For a larger shear rate of  $\dot{\gamma}^* = 1.84$ , the tumbling continues intermittently.

K-S theory [3, 4] explains the  $\eta_{\text{mb}}^*$ -dependence of the stability of tank-treading (compare Fig. 1), but cannot be applied to describe the dynamics, including morphological changes. We suggest the simple equations

$$\zeta_\alpha \dot{\alpha} = -\kappa^{-1} \partial F / \partial \alpha + A \dot{\gamma}^* \sin(2\theta) \quad (4)$$

$$\dot{\theta} = 0.5 \dot{\gamma}^* \{-1 + B(\alpha) \cos(2\theta)\}. \quad (5)$$

The force  $\partial F / \partial \alpha$  is calculated from the free energy  $F(\alpha)$  of Fig. 2. The second term of Eq. (4) is the deformation force due to the shear flow. Its angular dependence can be derived from the shape equations of Ref. [5], while the

amplitude is assumed to be independent of the asphericity  $\alpha$  (to leading order). Eq. (5) is adopted from K-S theory [3, 4]. Here,  $B$  is a constant which depends on viscosities and ellipsoid shape. For  $B > 1$ , a steady angle  $\theta = 0.5 \arccos(1/B)$  exists and tank-treading motion occurs, while for  $B < 1$ , there is no stable angle and tumbling motion occurs. In our case, the vesicle shape can be time dependent, so that  $B$  is no longer constant. For simplicity, we assume a linear dependence of  $B$  on the asphericity,  $B(\alpha) = B_0 - B_1\alpha$ . To obtain tank-treading discocytes and tumbling prolate, we need  $B(0.2) > 1$  and  $B(0.7) < 1$ , respectively. Then, Eqs. (4) and (5) reproduce the simulated dynamics very well, see Figs. 3 and 4. The vesicle is found, for example, to relax after some tumbling to a stable, tank-treading discocyte state at  $\dot{\gamma}^* = 1.84$ , and to relax to a limit-cycle oscillation at  $\dot{\gamma}^* = 2.76$ .

The vesicle deformation due to shear depends on the inclination angle  $\theta$ . Shear flow increases the elongation of a vesicle for  $0 < \theta < \pi/2$  (where  $\dot{\gamma}^* \sin(2\theta) > 0$ ), and the angles  $\theta$  of tank-treading motion belong to this region. On the other hand, shear flow reduces the elongation for  $-\pi/2 < \theta < 0$  (where  $\dot{\gamma}^* \sin(2\theta) < 0$ ) during tumbling. The force in the former case induces the discocyte-to-prolate transformation, in the latter case the prolate-to-discocyte transformation. With increasing membrane viscosity  $\eta_{mb}^*$ , the inclination angle  $\theta$  of a tank-treading discocyte decreases, and larger shear rates  $\dot{\gamma}^*$  are necessary to generate the required elongational forces to induce a discocyte-to-prolate transition.

It is also interesting to compare the effect of membrane viscosity  $\eta_{mb}$  and internal viscosity  $\eta_{in}$ . In both cases, an increase of the viscosity induces a decrease of the inclination angle  $\theta$  and a transition from tank-treading to tumbling. However, the effect of internal viscosity  $\eta_{in}$  is less dependent on the vesicle morphology. K-S theory [3] shows that the tank-treading phase of oblate vesicle is destabilized a little faster than that of prolate with an increase of  $\eta_{in}$  (for  $\eta_{mb}^* = 0$ ); the transition viscosity is  $\eta_{in}/\eta_0 = 2.8$  and  $3.3$  of oblate and prolate ellipsoids at  $V^* = 0.59$ , respectively. Thus, only a sufficiently high membrane viscosity  $\eta_{mb}^*$  can induce a prolate-to-discocyte transformation.

The membrane viscosity of human red blood cells is estimated from the analysis of the tank-treading motion to be  $\eta_{mb} = 10^{-7}$ Ns/m [4], while a micropipette recovery-time technique gives  $\eta_{mb} = 10^{-6}$ Ns/m [8]. When the viscosity of the external fluid is set to the same value of the intracellular fluid,  $\eta_0 = 10^{-2}$ Pa s, and  $R_0 = 3.3\mu\text{m}$ , the relative membrane viscosity is then found to be in the range  $\eta_{mb}^* = 1...10$ . Thus, the effect of this membrane viscosity is sufficiently large (compare Fig. 1) to strongly affect the dynamics of erythrocytes. The viscoelasticity of membrane can be changed by varying the chemical composition of the solvent [1]. It is difficult to separate the effects of viscosity and elasticity, however. On the

other hand, the membrane viscosity of polymersome can be changed by varying the polymer chain length. Thus, polymersomes seem to be very well suited to study the effect of membrane viscosity experimentally.

To summarize, we have applied the MPCD method to a vesicle with viscous membrane under a simple shear flow. The membrane viscosity qualitatively changes the vesicle dynamics. The shear induces a discocyte-to-prolate or prolate-to-discocyte transformation at low or high membrane viscosity, respectively. The deformations of other vesicles shapes, such as stomatocyte and budded vesicles, will be interesting subjects in the further studies.

We would like to thank N. Kikuchi (Oxford), A. Lamura (Bari), and R.G. Winkler for helpful discussions. HN's stay at FZJ was supported by the Postdoctoral Fellowships for Research Abroad of the Japan Society for the Promotion of Science (JSPS).

- 
- [1] S. Chien, *Ann. Rev. Physiol.* **49**, 177 (1987).
  - [2] T. M. Fischer, M. Stöhr-Liesen, and H. Schmid-Schönbein, *Science* **202**, 894 (1978).
  - [3] S. R. Keller and R. Skalak, *J. Fluid Mech.* **120**, 27 (1982).
  - [4] R. Tran-Son-Tay, S. P. Suter, and P. R. Rao, *Biophys. J.* **46**, 65 (1984).
  - [5] M. Kraus, W. Wintz, U. Seifert, and R. Lipowsky, *Phys. Rev. Lett.* **77**, 3685 (1996).
  - [6] J. Beaucourt *et al.*, *Phys. Rev. E* **69**, 011906 (2004).
  - [7] C. Pozrikidis, *Annals Biomed. Eng.* **31**, 1194 (2003).
  - [8] G. B. Nash and H. J. Meiselman, *Biophys. J.* **43**, 63 (1983).
  - [9] K. Tsukada, E. Sekizuka, C. Oshio, and H. Minamitani, *Microvasc. Res.* **61**, 231 (2001).
  - [10] B. M. Discher *et al.*, *Science* **284**, 1143 (1999).
  - [11] R. Dimova *et al.*, *Eur. Phys. J. E* **7**, 241 (2002).
  - [12] A. Malevanets and R. Kapral, *J. Chem. Phys.* **110**, 8605 (1999).
  - [13] A. Malevanets and J. M. Yeomans, *Europhys. Lett.* **52**, 231 (2000).
  - [14] T. Ihle and D. M. Kroll, *Phys. Rev. E* **63**, 020201(R) (2001).
  - [15] N. Kikuchi, C. M. Pooley, J. F. Ryder, and J. M. Yeomans, *J. Chem. Phys.* **119**, 6388 (2003).
  - [16] N. Kikuchi, Ph. D. thesis, University of Oxford 2003.
  - [17] A. Lamura, G. Gompper, T. Ihle, and D. M. Kroll, *Europhys. Lett.* **56**, 319 (2001).
  - [18] M. Ripoll, K. Mussawisade, R. G. Winkler, and G. Gompper, preprint (2004).
  - [19] G. Gompper and D. M. Kroll, *J. Phys. Condens. Matter* **9**, 8795 (1997).
  - [20] W. Helfrich, *Z. Naturforsch.* **28c**, 693 (1973).
  - [21] G. Gompper and D. M. Kroll, *J. Phys. I (France)* **6**, 1305 (1996).
  - [22] M. P. Allen and D. J. Tildesley, *Computer simulation of liquids* (Clarendon Press, Oxford, 1987).
  - [23] H. Noguchi and G. Gompper, (in preparation).
  - [24] B. A. Berg, H. Noguchi, and Y. Okamoto, *Phys. Rev. E* **68**, 036126 (2003).
  - [25] J. Rudnick and G. Gaspari, *J. Phys. A* **19**, L191 (1986).